Published in final edited form as:
J Immunol. 2009 November 15; 183(10): 6460–6468. doi:10.4049/jimmunol.0900983.

Outside-In Signal Transmission by Conformational Changes in Integrin Mac-1[1]

Craig T. Lefort[2,*], **Young-Min Hyun**[2,*], **Joanne B. Schultz**[†], **Foon-Yee Law**[*], **Richard E. Waugh**[†], **Philip A. Knauf**[‡], and **Minsoo Kim**[3,*]

[*]Department of Microbiology and Immunology, David H. Smith Center for Vaccine Biology and Immunology, University of Rochester, Rochester, NY 14642

[†]Department of Biomedical Engineering, University of Rochester, Rochester, NY 14642

[‡]Department of Biochemistry and Biophysics, University of Rochester, Rochester, NY 14642

Abstract

Intracellular signals associated with or triggered by integrin ligation can control cell survival, differentiation, proliferation, and migration. Despite accumulating evidence that conformational changes regulate integrin affinity to its ligands, how integrin structure regulates signal transmission from the outside to the inside of the cell remains elusive. Using fluorescence resonance energy transfer, we addressed whether conformational changes in integrin Mac-1 are sufficient to transmit outside-in signals in human neutrophils. Mac-1 conformational activation induced by ligand occupancy or activating Ab binding, but not integrin clustering, triggered similar patterns of intracellular protein tyrosine phosphorylation, including Akt phosphorylation, and inhibited spontaneous neutrophil apoptosis, indicating that global conformational changes are critical for Mac-1-dependent outside-in signal transduction. In neutrophils and myeloid K562 cells, ligand ICAM-1 or activating Ab binding promoted switchblade-like extension of the Mac-1 extracellular domain and separation of the α_M and β_2 subunit cytoplasmic tails, two structural hallmarks of integrin activation. These data suggest the primacy of global conformational changes in the generation of Mac-1 outside-in signals.

Neutrophils, or polymorphonculear leukocytes (PMNs),[4] play key roles in the host defense network against pathogens by virtue of their abilities to phagocytose microorganisms and to produce reactive oxygen intermediates and proteolytic enzymes. To fight invading microorganisms, PMNs must exit the blood stream and travel to the site of inflammation. The rapid recruitment of PMNs in response to an inflammatory cue is enabled by the capture and firm adhesion of PMNs to the endothelial cell lining of the blood vessel lumen, a process primarily mediated by β_2 integrins (1). Leukocyte adhesion deficiency, caused by the absence or mutation of the β_2 integrin subunit, results in enhanced susceptibility to bacterial infection, neutrophilia, skin lesions, and impaired wound healing (2,3).

[1]This work was supported by National Institutes of Health Grants IH HL087088 (to M.K.) and HL18208 (to M.K. and R.E.W.).

3Address correspondence and reprint requests to Dr. Minsoo Kim, Department of Microbiology and Immunology, David H. Smith Center for Vaccine Biology and Immunology, Rochester, NY 14642. minsoo_kim@urmc.rochester.edu.

[2]These authors contributed equally to this work.

Disclosures

The authors have no financial conflict of interest.

[4]Abbreviations used in this paper: PMN, polymorphonuclear leukocyte; PVP, polyvinylpyrrolidone; ORB, octadecylrhodamine B; FP, fluorescent protein; CFP, cyan FP; mCFP, monomeric CFP; YFP, yellow FP; mYFP, monomeric YFP; EM, electron microscopy; FRET, fluorescence resonance energy transfer.

Integrins are heterodimeric transmembrane receptors consisting of α and β subunits that mediate cell-cell adhesion and cell adhesion to the extracellular matrix (4). Integrins mediate bidirectional communication between the extracellular environment and the cytoplasm and thus regulate a broad array of cellular processes. Nearly one-half of the 24 distinct integrin pairs, including all of the β_2 integrins found exclusively on leukocytes, contain a ligand binding inserted (I) domain located in the headpiece of the α subunit (5). In PMNs, Mac-1 ($\alpha_M\beta_2$, CR3, or CD11b/CD18) is perhaps the most widely studied integrin with respect to PMN migration (6) and phagocytosis (7). Mac-1 binds to a wide range of ligands, including ICAM-1 (8), fibrinogen (9), and C3 fragment iC3b (10). Whereas integrins on circulating PMNs primarily exist in a nonadhesive basal state, various activators, including bacterial products such as fMLP and tissue factors such as TNF-α, rapidly increase the cell surface density of Mac-1 and its affinity for extracellular ligands, including sites on endothelial cells that line the blood vessel interior (11).

The rapid up-regulation of integrin affinity in the presence of chemokines or other activating factors is mediated by inside-out signals (4). During inside-out activation, intracellular signaling induces the binding of cytoplasmic proteins, such as talin, to the short integrin tail. Protein binding to the integrin tail presumably destabilizes the association of the α and β integrin subunit and causes conformational rearrangements that are propagated to the extracellular portion of the integrin (5). These structural changes ultimately result in extension of the headpiece away from the cell surface in a switchblade-like motion and separation of the cytoplasmic tails of the α and β integrin subunits (5,12).

Structural and functional studies suggest that integrins exist in a dynamic equilibrium between three different affinity states: low, intermediate, and high (5). The low affinity state is characterized by a compact structure in which the extracellular domain is bent over and the integrin headpiece is in close proximity to the cell membrane, with the cytoplasmic tails of the α and β subunits closely apposed (13). The intermediate affinity integrin exhibits an extended headpiece, but the ligand binding I domain in the α subunit is in a closed conformation. A downward shift of the α I domain α7 helix and subsequent swing-out of the β_2 hybrid domain leads to the high-affinity state (13,14). Mutational studies using engineered disulfide bonds to lock LFA-1 (integrin $\alpha_L\beta_2$) in different affinity states indicate that binding to ICAM-1 is increased ~500-fold for the intermediate-affinity state and ~10,000-fold for the high-affinity state (14).

Ligand binding, which also triggers integrin conformational changes, is involved in integrin-dependent outside-in signals. Outside-in signaling can affect a variety of cellular functions such as apoptosis, cytotoxicity, cell proliferation, cytokine production, Ag presentation, and gene activation (15,16). Separation of the $\alpha_{IIb}\beta_3$ transmembrane domains has been shown to be required for outside-in signaling and subsequent cell spreading (17), suggesting that integrin conformational change is important for signal generation. Interestingly, the downward displacement of the α7 helix in the α subunit I domain that occurs during integrin activation is also observed in response to ligand binding in the absence of activation (18). These data indicate that inside-out activation and outside-in signaling may involve the same structural changes in the I domain (5). Therefore, we hypothesize that the active, high-affinity conformation is sufficient to induce outside-in signaling and that ligand occupancy merely shifts the conformational equilibrium toward the fully active state of the integrin. This hypothesis is supported by experimental data from the therapeutic use of ligand-mimetic integrin antagonists. In the case of integrin $\alpha_{IIb}\beta_3$, ligand-mimetic antagonists have paradoxically enhanced integrin function and worsened some clinical outcomes (19,20). Although ligand-mimetic integrin antagonists block ligand binding, they also may induce conformational changes and, thus, initiate outside-in integrin signaling. In the current study, we found that Mac-1 activation stimulated by the Ab CBR LFA-1/2 is sufficient for the

generation of outside-in signals even in the absence of ligand binding, and developed a system to demonstrate that both CBR LFA-1/2 and ligand ICAM-1 induce conformational changes associated with integrin activation in live cells.

Materials and Methods

Reagents and Abs

Polymorph cell separation medium was obtained from Accurate Chemical and Scientific. BSA, polyvinylpyrrolidone (PVP), fMLP, PMA, PI3K inhibitor LY294002, and p38/MAPK inhibitor SB239063 were from Sigma-Aldrich. Octadecylrhodamine B (ORB) was purchased from Invitrogen. Annexin V-FITC was from Southern Biotech. ICAM-1 and IL-8 were purchased from R&D Systems.

The following Abs were used: FITC anti-human CD11b clone ICRF44 (8.9 FITC/IgG molar ratio; Ancell); FITC anti-human CD11b clone CBRM1/5 (4.5 FITC/IgG; eBioscience, or 5.7 FITC/IgG; BioLegend); FITC anti-CD11b clone VIM12 (Caltag Laboratories); anti-CD11b clone 44 (American Type Culture Collection); FITC IgG1 isotype control (Beck-man Coulter Immunotech); anti-phosphotyrosine (Millipore); anti-β-actin (Sigma-Aldrich); anti-p38 (pThr180/pTyr182 and pan-p38; Cell Signaling Technology); anti-Akt (pThr308 and pan-Akt; Cell Signaling Technology); polyclonal anti-GFP (Invitrogen); HRP-conjugated rabbit anti-mouse and goat anti-rabbit IgG (Zymed); and goat anti-mouse $F(ab')_2$ (Southern Biotech). Anti-β_2 CBR LFA-1/2 mAb and TS1/18 mAb were provided by T. Springer (CBR Institute for Biomedical Research, Boston, MA).

DNA plasmids and constructs

α_M-monomeric cyan fluorescent protein (mCFP) and β_2-monomeric yellow fluorescent protein (mYFP) were generated using the mammalian expression vectors pECFP-N1 and pEYFP-N1 (ClonTech), respectively, in which Leu^{221} was replaced with lysine to produce the mono-meric mutant (21). Design of the β_2-mYFP construct has been described (12). For α_M-mCFP, PCR extension was performed using cDNA of the wild-type α_M subunit (GenBank accession number BC096346) as a template with the upstream primer 5′-ATATAGCTAGCTGCCACCAT GGCTCTCAGAGTCCTTCT-3′ with an *Nhe*I site and the downstream primer 5′-TATATCCGCGGCGCGGGTTCCGGAGCCTGGGGTTCGGC CCCCGGCCCA-3′ with a *Sac*II site. A linker between α_M and enhanced CFP was designed based on the polyproline II helix (22) to provide flexibility between the CFP tag and the α_M integrin subunit. The PCR product was digested with *Nhe*I and *Sac*II and inserted into pECFP or into an α_4-mCFP construct (23) to make α_M-mCFP with a 15 or 25 amino acid linker, respectively. The 15 amino acid linker region sequence was APEPAPRARDPPVAT and the 25-aa linker region sequence was APEPAPRPTAAPEPAKRARDPPVAT. α_M-mCFP was then inserted into pCDNA3.1/Hygromycin (Invitrogen) using *Nhe*I and *Not*I digestion. Preliminary experiments indicated that linker regions of 25 and 6 aa produced optimal fluorescence resonance energy transfer (FRET) constructs for α_M-mCFP and β_2-mYFP, respectively.

Cell culture and transfection

Human PMNs were isolated from heparinized whole blood obtained from healthy donors using polymorph cell separation medium or Polymorphprep, as described in the manufacturer's instructions. Contaminating erythrocytes were eliminated by hypotonic lysis. Purified PMNs were suspended in either BSS (146 mM NaCl, 5 mM KCl, 1 mM $CaCl_2$, 1 mM $MgCl_2$, 5.5 mM D-glucose, 10 mM HEPES, pH 7.4) for flow cytometry experiments or L-15 media (Life Technologies) supplemented with 2 mg/ml D-glucose and 0.1% BSA for signaling and apoptosis assays.

K562 human leukemia cells were maintained in RPMI 1640 (Life Technologies) supplemented with 10% FBS, 100 μg/ml streptomycin, and 100 U/ml penicillin. To produce stable transfectants, K562 cells were transfected with 75 μg each of α_M-mCFP and β_2-mYFP expression constructs by electroporation at 250 V and 960 μF using cuvets with 0.4-cm path length (Bio-Rad). Transfected cells were cultured for 24 h in RPMI 1640 containing 20% FBS and then selected for resistance to 1 mg/ml G418 for 2 wk. K562 transfectants were sorted twice by immunofluorescence with anti-α_M clone ICRF44 and then seeded at a single cell per well in 96-well plates to obtain homogeneous and stable clones.

Flow cytometry FRET assay

Purified PMNs suspended at 1×10^7 cells/ml in BSS buffer containing 0.1% BSA, 1 mM $CaCl_2$, and 1 mM $MgCl_2$ (BSS+), and 100 μl of unstimulated cells were placed in cold 1.5-ml microcentrifuge tubes (Eppendorf) on ice for Ab labeling. Cells were treated with 10 nM fMLP for 15 min at 37°C and then placed on ice for Ab labeling. Each tube containing 1×10^6 cells was labeled with FITC-ICRF44 (9.8 μg/ml), FITC-VIM12 (9.5 μg/ml), or FITC-CBRM1/5 (15 μg/ml) for 45 min on a rotating platform at 4°C, except FITC-CBRM1/5 which was labeled for 60 min at 4°C. All tubes were then washed three times with BSS+ buffer, and 2×10^6 cells were resuspended in 1 ml of the same buffer. Ice cold Ab-labeled PMNs (250 μl; 5×10^5 cells) were placed in 250 μl of cold buffer in a snap cap culture tube (Falcon), kept on ice, and analyzed by flow cytometry on a FACSCalibur (BD Biosciences). At timed intervals, ORB was added to a set of four tubes containing Ab-labeled cells or cells alone on ice so that the final concentrations are 0, 75, 200, and 400 nM ORB. Each tube was mixed and kept on ice for 20 min before reading on the flow cytometer. Analysis was done by gating on the PMN population, and 10,000 cells were analyzed for each sample using FlowJo software (Tree Star).

Transfer of energy from the FITC donor to the rhodamine acceptor causes a decrease in the fluorescence intensity in the FITC channel. The relation between the decrease in FITC intensity and the amount of ORB in the membrane depends on the distance between the FITC donor and the membrane surface, *L*, to the inverse fourth power (24):

$$F_{DA} = F_D / (1 + S[\mathrm{ORB}]) \tag{1}$$

where

$$S = \pi R_0^6 / 2L^4,$$

and where F_{DA} is the donor (FITC) fluorescence in the presence of acceptor (ORB), F_D is the donor fluorescence in the absence of acceptor, [ORB] is the concentration of acceptor in the cell membrane (assumed to be proportional to the ORB fluorescence), and *S* is the slope factor, which depends on the Forster radius (R_0) and distance between donor and acceptor (*L*). For two different donors, or a donor under different conditions, the distance ratios for the two conditions are related to the slopes for those conditions by

$$L_1 / L_2 = (S_1 / S_2)^{1/4} \tag{2}$$

Cytoplasmic tail FRET assay

Before image acquisition, K562 cells expressing α_M-mCFP and β_2-mYFP were washed twice and then resuspended in L-15 medium supplemented with 2 mg/ml D-glucose. Cells

were allowed to settle on PVP-coated coverslips and then treated with activating agents at room temperature, except for PMA treatment, which was performed at 37°C. Initial images were acquired 10 min after treatment.

Imaging was performed with a Nikon Eclipse E2000-E microscope using a 60 × oil immersion objective coupled to a QuantEM charge-coupled device camera (Roper Scientific). The following imaging filters were from Chroma: YFP (HQ500/20X, Q515LP, HQ535/30M), CFP (D436/20X, 455DCLP, D480/40M), and YFP Photobleach (D535/50X; dichroic full mirror, metal slug). Image acquisition, background subtraction, and data analysis were performed using Nikon NIS-Element software. Cells were imaged with a 120-W mercury arc lamp of the X-Cite 120 XL system (EXFO Photonic Solutions) through a ND8 filter for CFP and YFP images, and without ND filters for YFP Photobleach. Exposure time was 0.1 s for both CFP and YFP, with 2 × 2 binning, and 3 min for photobleaching, resulting in a 90% reduction in YFP fluorescence intensity. CFP and YFP images were taken both before and after YFP acceptor photobleaching. Image analysis was performed on the signal from the cell membrane ring. After background subtraction, FRET efficiency (*E*) was calculated as (25)

$$E=1-(F_{\mathrm{CFP}}(d)_{\mathrm{Pre}}/F_{\mathrm{CFP}}(d)_{\mathrm{Post}})(25),$$

where $F_{\mathrm{CFP}}(\mathrm{d})_{\mathrm{Pre}}$ and $F_{\mathrm{CFP}}(\mathrm{d})_{\mathrm{Post}}$ are the mean CFP emission intensities before and after YFP photobleaching. For each experimental condition, four to nine cells were analyzed over at least three different experiments.

Cell adhesion assay

Corning 96-well tissue culture plates were coated with 10 μg/ml ICAM-1/Fc (R&D Systems). K562 cells expressing α_M-mCFP and β_2-mYFP were washed and resuspended in L-15 medium containing 2 mg/ml D-glucose, and 1×10^5 cells in 0.1 ml volume were added to each well. Cells were allowed to adhere for 30 min. Plates were then washed gently, and the number of adherent cells per field was counted.

Flow cytometry, immunoprecipitation, and immunoblotting

Flow cytometry was performed as described (12). Mac-1 was detected using anti-α_M ICRF44 mAb and anti-β_2 TS1/18 mAb, followed by R-PE-conjugated anti-mouse IgG.

K562 cells expressing α_M-mCFP and β_2-mYFP were lysed on ice for 30 min in lysis buffer (HBSS; Life Technologies) containing 60 mM *n*-octyl-β-D-glucopyranoside, 1% Triton X-100, 1 mM calcium chloride, 1 mM magnesium chloride, and 2 mM sodium orthovanadate, Complete protease inhibitor mixture (Roche). For immunoprecipitation of β_2 integrins; 4 μg of CBR LFA-1/2 mAb were used. Proteins were separated on a SDS-PAGE gel and either silver stained or transferred to nitrocellulose for immunoblotting. Polyacrylamide gels were Silver stained with a Silver Express Kit (Invitrogen). Immunoblots were probed with the indicated Abs in Trisglycine, SDS buffer (Bio-Rad) containing 0.1% Tween 20 (GE Healthcare Biosciences), and 1% BSA. Western blots were quantified using the ImageJ (National Institutes of Health) software gel plotting macro.

Apoptosis assays

Purified PMNs were suspended at 2×10^6 cells per ml in L-15 medum (Life Technologies) supplemented with 2 mg/ml D-glucose and 0.1% BSA. After either a 4-h (in the presence of 10 ng/ml TNF-α) or 16-h treatment at 37°C, cells were placed on ice, washed twice with PBS containing 1 mM $CaCl_2$ and 1 mM $MgCl_2$, and then labeled with annexin V-FITC for

15 min. Flow cytometry analysis was done by gating on the PMN population, and 10,000 cells were analyzed for each sample using FlowJo software. Data are presented as mean ± SEM from three experiments performed in duplicate and are expressed as percent of annexin V-positive cells.

Data analysis

Data are presented as the mean ± SEM. A two-tailed Student *t* test was performed to determine the statistical significance of differences between groups, and *p* values are indicated in figure legends.

Results

Ab-induced Mac-1 activation and outside-in signaling

Inside-out integrin activation involves conformational rearrangement of both the intracellular and extracellular domains, resulting in a large increase in ligand affinity. The prevailing dogma has been that outside-in signaling is driven by integrin clustering (26,27), a consequence of multivalent ligand binding (28). However, recent studies demonstrate that conformational separation of the α and β subunit transmembrane domains and, presumably, cytoplasmic tails is required for $\alpha_{IIb}\beta_3$ integrin-mediated outside-in signaling (17). In addition, inside-out activation and ligand binding in the absence of activation induce similar structural changes within the I domain (5). Therefore, integrin headpiece extension and tail separation, the conformational changes that occur during activation, may be sufficient for outside-in signal generation. If this is indeed the case, intracellular signal transduction in response to ligand binding (outside-in signaling) may be the result of a shift in the conformational equilibrium toward the fully active state of the integrin. This hypothesis also could predict that other reagents that similarly shift the conformational equilibrium toward the active structure should produce outside-in signals.

CBR LFA-1/2 is a mAb that recognizes the I-EGF3 domain of the β_2 integrin subunit and induces activation (29,30). To determine whether CBR LFA-1/2 initiates outside-in signaling in the absence of ligand binding, overall intracellular protein tyrosine phosphorylation of human PMNs was analyzed. In these experiments, CBR LFA-1/2 Fab fragments were used to avoid potential signaling caused by FcR interactions or Ab-induced Mac-1 lateral association, and anti-α_M Fab fragments were used to block homotypic PMN interaction through the binding of the α_M I domain with ICAM-1. As shown in Fig. 1*A*, CBR LFA-1/2 stimulated broad protein tyrosine phosphorylation to an extent similar to that of human ICAM-1. To determine whether Mac-1 clustering alone, in the absence of activation, generates outside-in signals, Mac-1 was cross-linked using anti-α_M (clone 44) Fab fragments (Fab44) and secondary $F(ab')_2$ (Fig. 1*B*). Others have shown that the anti-α_M (clone 44) mAb stabilizes the inactive Mac-1 conformer (31), and our studies also indicate that Fab44 inhibits the exposure of the activation-dependent KIM127 mAb epitope (supplemental Fig. 1).[5] Mac-1 clustering produced only a modest increase in tyrosine phosphorylation (Fig. 1*A*). These data suggest that activation of Mac-1 using Abs, but not clustering, is sufficient to induce outside-in signaling in PMNs that mimics that produced by physiological ligand binding.

PMNs play a critical role in host defense by engulfing and destroying pathogens and microbes. Under normal conditions, PMNs undergo constitutive apoptosis and thus exhibit a relatively short half-life. During inflammation, however, prosurvival signals delay PMN apoptosis (32). Mac-1-dependent signaling has been implicated as an important regulator of

[5]The online version of this article contains supplemental material.

PMN apoptosis. Two different Mac-1 outside-in signaling pathways have been shown to regulate PMN apoptosis; the PI3K-Akt pathway and p38 MAPK (p38/ MAPK)-ERK pathway (32,33). We found that Mac-1 activation by CBR LFA-1/2 induces both p38/ MAPK and PI3K/Akt signaling, as determined by Western blot with Abs specific to phosphorylated p38 and Akt (Fig. 1*C*). ICAM-1 treatment activated Akt, but not p38, whereas Mac-1 clustering did not induce activation of either pathway (Fig. 1*C*).

As CBR LFA-1/2 was able to induce p38/MAPK and PI3K/Akt, we sought to determine whether CBR LFA-1/2 prolongs PMN lifespan. Cells were treated for 16 h with CBR LFA-1/2, ICAM-1, or Fab44 and secondary cross-linking $F(ab')_2$ to cluster Mac-1, in the absence and presence of the PI3K inhibitor LY294002 or the MAPK inhibitor SB239063. Under control conditions, 85.6% of PMNs were apoptotic, as determined by positive staining for annexin V. Treating PMN with CBR LFA-1/2 or ICAM-1, but not clustering reagents, significantly inhibited constitutive apoptosis (Fig. 1*D*). However, both the PI3K inhibitor LY294002 and MAPK inhibitor SB239063 failed to reverse the inhibition (Fig. 1, *D* and *E*). These data indicate that outside-in signaling induced by conformational activation of Mac-1 through CBR LFA-1/2 binding is sufficient to regulate constitutive PMN apoptosis in a manner independent of PI3K/Akt and p38/MAPK activation.

Extension of the Mac-1 extracellular domain

The experiments described above demonstrate that CBR LFA-1/2 stimulates outside-in signaling in PMNs, similar to that of the physiological ligand ICAM-1 binding. Integrin activation is associated with conformational opening of the extracellular domain, as suggested by the wide range of mAbs that specifically recognize extracellular epitopes of the activated or ligand-bound integrin (29). The switchblade-like conversion of cell surface integrins from a compact bent structure to an extended form under artificial activating conditions has been observed using electron microscopy (EM; Ref. 13). Furthermore, unbending of the integrins VLA-4 (34) and LFA-1 (35) in response to activation of live cells has been demonstrated by FRET using flow cytometry. To address confor-mational changes in Mac-1 induced by various activation conditions, we have made measurements of Mac-1 extracellular domain extension on primary human PMNs by observing energy transfer between fluorophore-conjugated Abs and a membrane dye (Fig. 2*A*).

To investigate specific and regulated conformational changes in the α and β subunit extracellular domains in Mac-1, we developed a flow cytometry-based FRET method that can provide information about the relative distance between a fluorescently labeled mAb attached to the α_M I domain (FITC-ICRF44; donor, D) and lipid-soluble acceptor fluorophores (ORB; acceptor, A) that have partitioned into the lipid bilayer (Fig. 2*B*). Donor fluorophores in close proximity to acceptor fluorophores will be quenched to a greater extent than those that are more distal. Fig. 2*B* shows that the variation in ICRF44 staining and ORB uptake among PMNs is small, exhibiting very narrow peaks in fluorescence intensity. Increasing concentrations of the ORB acceptor incorporated into the cell membrane and resulted in the quenching of donor fluorescence in the FITC channel (Fig. 2*C* and supplemental Fig. 2, *A* and *B*). The mean fluorescence intensity of cells labeled with donor FITC-conjugated mAbs and acceptor ORB dye was measured using flow cytometry. When plotted as donor fluorescence vs acceptor fluorescence (supplemental Fig. 2*B*), the data fit well to Equation 1 with highly reproducible slope factors, *S*, that are a quantitative measure of the extent of energy transfer from the donor to the acceptor fluorophore. To normalize the data for the Mac-1 expression level, the ratio of initial donor fluorescence (F_D) to donor fluorescence in the presence of acceptor (F_{DA}) are plotted vs acceptor (ORB) fluorescence (Fig. 3*A* and supplemental Fig. 2*B*).

For ICRF44, a nonselective mAb directed against the α_M I domain that recognizes both the active and inactive integrin (36), increasing concentrations of the FRET acceptor, ORB, quenched the donor FITC fluorescence in untreated and fMLP-treated cells (Fig. 3*A*). The distance ratio (L_2/L_1,Equation 2), a metric indicating the change in donor-acceptor separation, for fMLP-stimulated vs unstimulated cells was calculated to be 1.23 ± 0.02 (n = 13) for the ICRF44-labeled Mac-1 population. Because fMLP enhances the cell surface expression of Mac-1, we also tested the activation of only the Mac-1 population at the cell surface before stimulation by labeling cells with FITC-ICRF44 before fMLP treatment and observed a distance ratio comparable with that found for the entire Mac-1 population (data not shown). In addition, similar distance ratios for ICRF44 were observed in cells treated with the chemokine IL-8 or phorbol ester (Fig. 4). Given that the headpiece of the activated integrin is hypothesized to be positioned >200 Å from the membrane (13), a distance at which there is no FRET, these data suggest that physiological stimulation activates only a subpopulation of cell surface Mac-1, consistent with previous studies (37). Activation of only 10% of the Mac-1 population in response to fMLP is sufficient to substantially change PMN adhesiveness (37). Under these conditions, the decrease in FRET signal for the activated form of Mac-1 would be dampened by the large fraction of the Mac-1 population that remains inactive. Therefore, to measure the changes in FRET that are contributed exclusively from the active form of Mac-1, we used a mAb that selectively binds to active Mac-1, CBRM1/5 (Fig. 3*B*). Comparing the Ab-membrane distance of Mac-1 molecules labeled with CBRM1/5 under activating conditions with unstimulated cells labeled with ICRF44 results in a distance ratio of 1.58 ± 0.08 (n = 6), indicating that the active integrin has its headpiece more distal from the membrane. The decrease in energy transfer in CBRM1/5 after fMLP treatment is not due to the low donor intensity given that FRET can be detected at relatively low donor concentrations (supplemental Fig. 2*B*, FITC-ICRF44 unstimulated: donor intensities from 230 to 103 arbitrary fluorescence units; supplemental Fig. 2*C*, FITC-ICRF44 unstimulated: donor intensities from 61 to 7 arbitrary fluorescence units). The significantly greater distance ratio for CBRM1/5 compared with ICRF44 also supports the idea that only a subset of Mac-1 is activated in response to fMLP. In contrast, the distance ratio of VIM12, a mAb directed against the C-terminal portion of the α_M ectodomain which is predicted to experience no change in distance from the membrane during integrin headpiece extension, was 0.99 ± 0.02 (n = 5) for fMLP- or CBR LFA-1/2-activated vs resting PMNs (Fig. 5), confirming that PMN activation does not alter incorporation of the membrane dye. In addition, Fig. 5 shows that varying the donor signal intensity does not significantly affect the slope of the donor-acceptor curve. Together, these results indicate that inside-out integrin activation causes the Mac-1 headpiece to extend away from the cell membrane. Furthermore, these data validate the use of FRET between FITC-conjugated reagents and ORB to study conformational changes in the extracellular domain of Mac-1 on human PMNs.

It is thought that inside-out signaling induces the extension of the extracellular portion of the integrin and that subsequent ligand binding stabilizes the fully active conformation (13,38). Similarly, EM studies suggest that activating Abs shift the conformational equilibrium of the integrin toward its active, extended structure by sterically hindering the bent conformer (39). However, it is unclear whether Ab-induced activation involves a similar extension of the integrin extracellular domain on the living cell surface. To determine whether CBR LFA-1/2 stimulates Mac-1 extension, cells were exposed to CBR LFA-1/2 in the presence of Mn^{2+}. CBR LFA-1/2 stimulated Mac-1 headpiece extension, decreasing the quench of FITC-ICRF44 by ORB (Fig. 3*C*) and resulting in a distance ratio of 1.29 ± 0.06 (n = 3). Exposure to 1 mM Mn^{2+} alone did not affect FRET between FITC-ICRF44 and ORB (data not shown). Labeling CBR LFA-1/2-activated cells with FITC-conjugated CBRM1/5 (Fig. 3*D*) and computing the donor-acceptor separation vs FITC-ICRF44-labeled resting cells result in a distance ratio of 1.52 ± 0.08 (n = 3). When FITC-labeled ICAM-1 was used as a donor

fluorophore (Fig. 3*E*), incubation with CBR LFA-1/2 resulted in a distance ratio of 1.68 ± 0.07 (n = 3), indicating that ligand-bound Mac-1 is in its extended form. Together, these data suggest that activation of Mac-1 by physiological ligand binding or by activating Abs results in the extension of the Mac-1 extracellular domain.

Separation of Mac-1 cytoplasmic tails

Inside-out activation of integrins through cell surface receptors induces the recruitment of effector proteins to the integrin cytoplasmic domains. Binding of intracellular proteins, such as talin, induces the spatial separation of the α and β integrin subunit tails (12). Extracellular activation of integrins by binding of mAb or ligand also causes conformational separation of integrin tails (12). The loss of FRET between fluorescent protein (FP)-tagged integrin subunits has been used to demonstrate that the C-termini of LFA-1 move apart in response to activation or ligand binding (12). To investigate whether Mac-1 undergoes similar integrin cytoplasmic tail separation during activation, constructs consisting of α_M fused to mCFP and β_2 fused to mYFP were stably transfected into the human myeloid leukemic K562 cell line (K562/α_M-mCFP/β_2-mYFP). FP-tagged Mac-1 was expressed on the surface of K562 cells, as shown using flow cytometry (Fig. 6*A*), and the fluorescence signal localized to the cell membrane (Fig. 6*B*). Biochemical analyses demonstrate that there is minimal proteolysis of the FP tags (Fig. 6*C*) and that α_M-mCFP and β_2-mYFP form a dimer (Fig. 6*D*). Activation of Mac-1 with Mn^{2+} and CBR LFA-1/2 enhanced the adhesion of K562/α_M-mCFP/β_2-mYFP cells to immobilized ICAM-1 (Fig. 6*E*), indicating that FP-tagged Mac-1 retains its normal adhesive function.

To determine the spatial separation between the FP-tagged cytoplasmic tails of Mac-1 (Fig. 7*A*), we measured the FRET signal using the acceptor photobleaching method (12). For each K562/α_M-mCFP/β_2-mYFP cell in suspension, the intensity of the CFP and YFP signal at the peripheral cell membrane was measured before and after photodestruction of the YFP fluorophore. In unstimulated cells, the FRET efficiency between the acceptor, α_M-mCFP, and donor, β_2-mYFP, was 0.20 ± 0.01 (Fig. 7*B*), similar to the FRET efficiency previously observed between α_L-mCFP and β_2-mYFP (12). Treatment with the Mac-1-activating CBR LFA-1/2 Fab fragment or the Mac-1 ligand ICAM-1, both in the presence of Mn^{2+}, caused a significant decrease in FRET efficiency (Fig. 7*B*), indicating an increase in the distance between the integrin cytoplasmic tails. Likewise, the inside-out integrin activator PMA induced a decrease in FRET (Fig. 7*B*), suggesting that intracellular conformational separation of the α_M and β_2 C termini leads to an increase in the affinity of the extracellular ligand binding α_M I domain. As seen previously for LFA-1 (12), Mn^{2+} treatment alone did not significantly alter the FRET efficiency between α_M-mCFP and β_2-mYFP (Fig. 7*B*). These data indicate that binding of activating mAb or physiological ligand induces conformational separation of the Mac-1 cytoplasmic tails. Taken together with the results demonstrating that CBR LFA-1/2 induces outside-in signaling in PMNs, these data suggest that global conformational activation of Mac-1 is sufficient to trigger intracellular signaling pathways.

Discussion

The structural mechanisms of integrin-mediated outside-in signal transmission are unclear. This study used a pair of FRET methods to show that activating Abs induce global conformational changes in the integrin that are sufficient for initiating intracellular signaling pathways. Determining the structural mechanisms of outside-in signaling is important as many antiadhesive therapeutics function as integrin ligand-mimetic competitive inhibitors. Therefore, small-molecule integrin inhibitors not only interfere with ligand binding but also stabilize particular integrin conformations. In addition, α/β I-like allosteric antagonists of β_2 integrins, such as XVA143 (14), inhibit structural communication between the α subunit I

domain and β subunit I-like domain, leaving the I domain in the low energy, inactive, closed conformation. At the same time, the α/β I-like allosteric antagonists stabilize the I-like domain in its active configuration. As a consequence of I-like domain activation, the α/β I-like allosteric antagonists stabilize the extracellular domain of the integrin in its extended conformation. Therefore, the induction of an active integrin conformation by nonphysiological ligands or by small-molecule antagonists raises the question of whether they could trigger outside-in signaling in a manner similar to that of natural ligands, thus stimulating the release of damaging reactive oxygen species and proteolytic enzymes. In the current study, we demonstrate that shifting the structural equilibrium of Mac-1 toward the fully active conformer, in which the extracellular domain is extended and the intracellular tails are separated, is sufficient for the generation of outside-in signals in human PMNs as detected by intracellular protein phosphorylation and annexin V staining.

The redistribution of Mac-1 and the regulation of its intracellular attachment to the actin cytoskeleton are crucial factors for PMN adhesion, shape change, and migration within the blood vessel lumen. With regard to outside-in signal generation, our studies do not define the role of active redistribution of Mac-1 during neutrophil polarization and migration; nonetheless, differential concentration of Mac-1 to the lamellapodium in polarized cells, a form of clustering, may work in concert with affinity regulation. Furthermore, regulation of the diffusiveness of Mac-1 may play an important role in adhesion strengthening. During normal recruitment, the binding of Mac-1 to counterreceptors on the endothelium, such as ICAM-1, is likely to be responsible for initiating outside-in signals. It is possible, however, that the shear stress that a leukocyte experiences during selectin-mediated rolling and subsequent adhesion can affect the conformation of an integrin (40,41). Although our studies were performed under conditions without physiological levels of shear stress, it would be interesting to determine whether integrin conformational changes induced by mechanical forces play a role in signal transmission during leukocyte recruitment.

In this study, we developed a system to monitor the activation state of Mac-1 in living cells by measuring the conformational state of the extracellular domain and of the cytoplasmic tails. Using FRET between Abs or ligands coupled to fluorophores and a membrane dye, our data demonstrate that the Mac-1 headpiece is located in close proximity to the cell surface in the basal, inactive state of the integrin. These data support previous EM studies indicating that unstimulated $\alpha_v\beta_3$ exists in a compact, bent-over conformation (13). Our work shows that the Mac-1 headpiece extends away from the membrane when integrins are activated by a physiological inside-out integrin activator, fMLP, as well as an artificial extracellular activator, CBR LFA-1/2 mAb. These results are in agreement with EM studies on LFA-1 and $\alpha_x\beta_2$, showing that CBR LFA-1/2 shifts the equilibrium toward the extended conformer (39).

FRET measurements were performed on PMNs labeled with two anti-α_M I domain mAbs: the nonselective ICRF44 and the active conformation-dependent CBRM1/5. We verified that the mAbs used did not cross-react with FcRs on the PMN surface using both mouse IgG1 isotype controls and FcR blocking reagents (data not shown). We were unable to effectively label Mac-1 with CBRM1/5 in unstimulated cells, indicating that relatively few Mac-1 molecules are in the active conformation in the basal state (data not shown). Even in cells activated with CBR LFA-1/2, the FITC-CBRM1/5 signal was lower than that of the other anti-Mac-1 FITC-conjugated Abs. The low fluorescence intensity of FITC-CBRM1/5-labeled cells did not affect the resolution of donor quenching, however, given that lowering the intensity of FITC-ICRF44 to levels similar to that of CBRM1/5 did not alter our ability to measure FRET in unstimulated cells (supplemental Fig. 2*C*).

In cells stimulated with fMLP, the FITC-ICRF44 donor fluorophore still exhibited acceptor dose-dependent quenching, suggesting that a significant fraction of Mac-1 molecules remains in an inactive conformation on the surface of stimulated cells. fMLP induced an ~5-fold increase in the expression of Mac-1 (data not shown), consistent with previous studies using PMNs (11). It is possible that the newly expressed Mac-1 reaches the cell surface in the inactive conformation, thus decreasing the effective distance ratio of the total Mac-1 population labeled with ICRF44. However, PMNs treated with the artificial extracellular activator CBR LFA-1/2, which does not affect Mac-1 expression, exhibit a similar distance ratio for both ICRF44 (1.29 for CBR LFA-1/2 vs 1.23 for fMLP) and CBRM1/5 (1.52 for CBR LFA-1/2 vs 1.58 for fMLP), suggesting that the large increase in Mac-1 surface expression in response to fMLP does not affect the conformational equilibrium of the entire cell surface Mac-1 population. Intact CBR LFA-1/2 mAb or Fab fragments, to prevent Ab-induced clustering, induced a similar unquenching of FITC-conjugated donor fluorophores (data not shown), suggesting that Mac-1 clustering does not alter the extension of the extracellular domain.

The binding of ICAM-1, a physiological ligand, to Mac-1 stabilizes the active conformer. In our studies, Mac-1 labeled with FITC-conjugated ICAM-1 in cells activated with CBR LFA-1/2 produced a distance ratio (1.68) that was not significantly different than that for CBRM1/5 (1.52). These results indicate that ICAM-1 binds primarily to active Mac-1 with its headpiece extended. Therefore, both ligand binding to Mac-1 and activation of Mac-1 by CBR LFA-1/2 mAb result in extension of the integrin headpiece.

We also used FRET to measure the separation of the Mac-1 cytoplasmic tails in response to activation. Basal measurements of FRET between α_M-mCFP and β_2-mYFP were similar to those for LFA-1 (12). Mac-1 activation by CBR LFA-1/2 or ICAM-1 binding caused a significant decrease in FRET efficiency, but not to the extent observed with LFA-1 (12). An explanation for the differences in FRET efficiency measurements between FP-tagged active LFA-1 and Mac-1 may lie in the lateral association of integrin molecules. We found that Mac-1 activation did not induce a significant decrease in FRET efficiency in K562 cells expressing high levels of α_M-mCFP and β_2-mYFP (data not shown), suggesting that FRET between FPs in adjacent Mac-1 dimers masks the decrease in FRET due to tail separation. Therefore, we chose a clone expressing relatively low levels of α_M-mCFP and β_2-mYFP to minimize the effects of receptor clustering on changes in FRET efficiency. Similar to LFA-1, the anti-β_2 activating CBR LFA-1/2 mAb, ICAM-1 binding, and inside-out activation by PMA treatment all induced Mac-1 tail separation. Taken together with the extracellular domain extension results, these data indicate that both the physiological ligand ICAM-1 and the artificial activator CBR LFA-1/2 induce similar global conformational changes in the Mac-1 molecule.

The binding of proteins that contain Src homology 2 domains with phosphotyrosine residues is a common platform for protein-protein interactions involved in signal transduction. Integrin-mediated outside-in signaling results in the tyrosine phosphorylation of a wide range of intracellular proteins, including focal adhesion kinase, Src family kinases, paxillin, and tensin (15). Recent evidence demonstrates that integrin conformational changes play an important role in integrin-dependent outside-in signaling (17), although it is not known whether global conformational rearrangements involved in integrin activation are sufficient to stimulate intracellular signaling pathways. Our data indicate that CBR LFA-1/2-induced changes in the structural conformation of Mac-1 enhance the phosphorylation of a broad range of proteins observed on a Western blot, including p38 and Akt, and leads to a similar level of overall phosphotyrosine as that stimulated by ligand-receptor binding. We used a recombinant monomeric form of ICAM-1 consisting solely of the extracellular domains of the molecule to show that clustering driven by multivalent ligand binding is not required for

the outside-in signaling. Likewise, Fab fragments of CBR LFA-1/2 and the anti-α_M blocking mAb 44 were used to ensure that Mac-1 clustering was not directly induced by Ab binding. However, these results do not preclude the possibility that Mac-1 activation alone could lead to clustering and, therefore, signal generation by enhancing homomeric interactions between subunits, as demonstrated with $\alpha_{IIb}\beta_3$ (42).

The induction of Mac-1-dependent outside-in signals in PMN by CBR LFA-1/2 has been observed previously (43). However, the investigators found that ligand binding was required for CBR LFA-1/2-induced p92 phosphorylation (43), suggesting that this signaling event was not a direct result of Mac-1 global conformational changes. Our results indicate that CBR LFA-1/2 enhances protein tyrosine phosphorylation even when the ligand binding site on the α_M I domain is blocked.

Constitutive PMN apoptosis has been shown to be regulated through Mac-1 outside-in signals (32). We show that outside-in signaling induced by both CBR LFA-1/2 and ICAM-1 delays PMN apoptosis. A recent study found that, in contrast to our results, constitutively active mutants of Mac-1 which stabilize the α_M I domain in its high affinity state do not confer the ability to prolong PMN lifespan (44). However, unlike CBR LFA-1/2, these mutations presumably do not affect the global conformation of Mac-1, including separation of the cytoplasmic tails. Therefore, it is not expected that locking the α_M I domain in its active conformation alone would induce outside-in signals.

In summary, we have found that a mAb, CBR LFA-1/2, that induces extension of the Mac-1 extracellular domain and spatial separation of the Mac-1 cytoplasmic tails, two hallmarks of full integrin activation, can trigger outside-in signaling in the absence of ligand binding. These results may explain the complications that have been observed in the clinic with ligand-mimetic integrin inhibitors. As such, the development of small-molecule inhibitors that block ligand recognition but do not stabilize active integrin conformers may provide more effective anti-adhesive therapies.

Supplementary Material

Refer to Web version on PubMed Central for supplementary material.

Acknowledgments

We thank Rachel Spoonhower and Pranita Sarangi for technical assistance.

References

1. Bunting M, Harris ES, McIntyre TM, Prescott SM, Zimmerman GA. Leukocyte adhesion deficiency syndromes: adhesion and tethering defects involving β_2 integrins and selectin ligands. Curr. Opin. Hematol 2002;9:30–35. [PubMed: 11753075]
2. Anderson DC, Schmalsteig FC, Finegold MJ, Hughes BJ, Rothlein R, Miller LJ, Kohl S, Tosi MF, Jacobs RL, Waldrop TC, et al. The severe and moderate phenotypes of heritable Mac-1, LFA-1 deficiency: their quantitative definition and relation to leukocyte dysfunction and clinical features. J. Infect. Dis 1985;152:668–689. [PubMed: 3900232]
3. Anderson DC, Springer TA. Leukocyte adhesion deficiency: an inherited defect in the Mac-1, LFA-1, and p150,95 glycoproteins. Annu. Rev. Med 1987;38:175–194. [PubMed: 3555290]
4. Hynes RO. Integrins: bidirectional, allosteric signaling machines. Cell 2002;110:673–687. [PubMed: 12297042]
5. Luo BH, Carman CV, Springer TA. Structural basis of integrin regulation and signaling. Annu. Rev. Immunol 2007;25:619–647. [PubMed: 17201681]

6. Ding ZM, Babensee JE, Simon SI, Lu H, Perrard JL, Bullard DC, Dai XY, Bromley SK, Dustin ML, Entman ML, Smith CW, Ballantyne CM. Relative contribution of LFA-1 and Mac-1 to neutrophil adhesion and migration. J. Immunol 1999;163:5029–5038. [PubMed: 10528208]
7. Dupuy AG, Caron E. Integrin-dependent phagocytosis: spreading from microadhesion to new concepts. J. Cell Sci 2008;121:1773–1783. [PubMed: 18492791]
8. Diamond MS, Staunton DE, de Fougerolles AR, Stacker SA, Garcia-Aguilar J, Hibbs ML, Springer TA. ICAM-1 (CD54): a counter-receptor for Mac-1 (CD11b/CD18). J. Cell Biol 1990;111:3129–3139. [PubMed: 1980124]
9. Altieri DC, Bader R, Mannucci PM, Edgington TS. Oligospecificity of the cellular adhesion receptor Mac-1 encompasses an inducible recognition specificity for fibrinogen. J. Cell Biol 1988;107:1893–1900. [PubMed: 3053736]
10. Beller DI, Springer TA, Schreiber RD. Anti-Mac-1 selectively inhibits the mouse and human type three complement receptor. J. Exp. Med 1982;156:1000–1009. [PubMed: 7153706]
11. Vedder NB, Harlan JM. Increased surface expression of CD11b/ CD18 (Mac-1) is not required for stimulated neutrophil adherence to cultured endothelium. J. Clin. Invest 1988;81:676–682. [PubMed: 3278004]
12. Kim M, Carman CV, Springer TA. Bidirectional transmembrane signaling by cytoplasmic domain separation in integrins. Science 2003;301:1720–1725. [PubMed: 14500982]
13. Takagi J, Petre BM, Walz T, Springer TA. Global conformational rearrangements in integrin extracellular domains in outside-in and inside-out signaling. Cell 2002;110 599-511.
14. Shimaoka M, Xiao T, Liu JH, Yang Y, Dong Y, Jun CD, McCormack A, Zhang R, Joachimiak A, Takagi J, Wang JH, Springer TA. Structures of the α_L I domain and its complex with ICAM-1 reveal a shape-shifting pathway for integrin regulation. Cell 2003;112:99–111. [PubMed: 12526797]
15. Berton G, Lowell CA. Integrin signalling in neutrophils and macrophages. Cell. Signalling 1999;11:621–635. [PubMed: 10530871]
16. Varga G, Balkow S, Wild MK, Stadtbaeumer A, Krummen M, Rothoeft T, Higuchi T, Beissert S, Wethmar K, Scharffetter-Kochanek K, Vestweber D, Grabbe S. Active MAC-1 (CD11b/CD18) on DCs inhibits full T-cell activation. Blood 2007;109:661–669. [PubMed: 17003381]
17. Zhu J, Carman CV, Kim M, Shimaoka M, Springer TA, Luo BH. Requirement of α and β subunit transmembrane helix separation for integrin outside-in signaling. Blood 2007;110:2475–2483. [PubMed: 17615290]
18. Emsley J, Knight CG, Farndale RW, Barnes MJ, Liddington RC. Structural basis of collagen recognition by integrin $\alpha_2\beta_1$. Cell 2000;101:47–56. [PubMed: 10778855]
19. Peter K, Schwarz M, Ylanne J, Kohler B, Moser M, Nordt T, Salbach P, Kubler W, Bode C. Induction of fibrinogen binding and platelet aggregation as a potential intrinsic property of various glycoprotein IIb/IIIa ($\alpha_{IIb}\beta_3$) inhibitors. Blood 1998;92:3240–3249. [PubMed: 9787160]
20. Quinn MJ, Plow EF, Topol EJ. Platelet glycoprotein IIb/IIIa inhibitors: recognition of a two-edged sword? Circulation 2002;106:379–385. [PubMed: 12119257]
21. Zacharias DA, Violin JD, Newton AC, Tsien RY. Partitioning of lipid-modified monomeric GFPs into membrane microdomains of live cells. Science 2002;296:913–916. [PubMed: 11988576]
22. Hasson MS, Muscate A, McLeish MJ, Polovnikova LS, Gerlt JA, Kenyon GL, Petsko GA, Ringe D. The crystal structure of benzoylformate decarboxylase at 1.6 Å resolution: diversity of catalytic residues in thiamin diphosphate-dependent enzymes. Biochemistry 1998;37:9918–9930. [PubMed: 9665697]
23. Hyun YM, Chung HL, McGrath JL, Waugh RE, Kim M. Activated integrin VLA-4 localizes to the lamellipodia and mediates T cell migration on VCAM-1. J. Immunol 2009;183:359–369. [PubMed: 19542447]
24. Holowka D, Baird B. Structural studies on the membrane-bound immunoglobulin E-receptor complex. 1. Characterization of large plasma membrane vesicles from rat basophilic leukemia cells and insertion of amphipathic fluorescent probes. Biochemistry 1983;22:3466–3474. [PubMed: 6225455]

25. Miyawaki A, Tsien RY. Monitoring protein conformations and interactions by fluorescence resonance energy transfer between mutants of green fluorescent protein. Methods Enzymol 2000;327:472–500. [PubMed: 11045004]
26. Miyamoto S, Akiyama SK, Yamada KM. Synergistic roles for receptor occupancy and aggregation in integrin transmembrane function. Science 1995;267:883–885. [PubMed: 7846531]
27. Yamada KM, Miyamoto S. Integrin transmembrane signaling and cytoskeletal control. Curr. Opin. Cell Biol 1995;7:681–689. [PubMed: 8573343]
28. Kim M, Carman CV, Yang W, Salas A, Springer TA. The primacy of affinity over clustering in regulation of adhesiveness of the integrin $\alpha_L\beta_2$. J. Cell Biol 2004;167:1241–1253. [PubMed: 15611342]
29. Lu C, Ferzly M, Takagi J, Springer TA. Epitope mapping of antibodies to the C-terminal region of the integrin β_2 subunit reveals regions that become exposed upon receptor activation. J. Immunol 2001;166:5629–5637. [PubMed: 11313403]
30. Petruzzelli L, Maduzia L, Springer TA. Activation of lymphocyte function-associated molecule-1 (CD11a/CD18) and Mac-1 (CD11b/CD18) mimicked by an antibody directed against CD18. J. Immunol 1995;155:854–866. [PubMed: 7608563]
31. Xiong JP, Li R, Essafi M, Stehle T, Arnaout MA. An isoleucine-based allosteric switch controls affinity and shape shifting in integrin CD11b A-domain. J. Biol. Chem 2000;275:38762–38767. [PubMed: 11034990]
32. Mayadas TN, Cullere X. Neutrophil β_2 integrins: moderators of life or death decisions. Trends Immunol 2005;26:388–395. [PubMed: 15922663]
33. Whitlock BB, Gardai S, Fadok V, Bratton D, Henson PM. Differential roles for $\alpha_M\beta2$ integrin clustering or activation in the control of apoptosis via regulation of akt and ERK survival mechanisms. J. Cell Biol 2000;151:1305–1320. [PubMed: 11121444]
34. Chigaev A, Buranda T, Dwyer DC, Prossnitz ER, Sklar LA. FRET detection of cellular alpha4-integrin conformational activation. Biophys. J 2003;85:3951–3962. [PubMed: 14645084]
35. Larson RS, Davis T, Bologa C, Semenuk G, Vijayan S, Li Y, Oprea T, Chigaev A, Buranda T, Wagner CR, Sklar LA. Dissociation of I domain and global conformational changes in LFA-1: refinement of small molecule-I domain structure-activity relationships. Biochemistry 2005;44:4322–4331. [PubMed: 15766261]
36. Zhang L, Plow EF. Amino acid sequences within the α subunit of integrin $\alpha_M\beta_2$ (Mac-1) critical for specific recognition of C3bi. Biochemistry 1999;38:8064–8071. [PubMed: 10387051]
37. Diamond MS, Springer TA. A subpopulation of Mac-1 (CD11b/ CD18) molecules mediates neutrophil adhesion to ICAM-1 and fibrinogen. J. Cell Biol 1993;120:545–556. [PubMed: 7678422]
38. Hantgan RR, Paumi C, Rocco M, Weisel JW. Effects of ligand-mimetic peptides Arg-Gly-Asp-X (X = Phe, Trp, Ser) on $\alpha_{IIb}\beta3$ integrin conformation and oligomerization. Biochemistry 1999;38:14461–14474. [PubMed: 10545168]
39. Nishida N, Xie C, Shimaoka M, Cheng Y, Walz T, Springer TA. Activation of leukocyte β_2 integrins by conversion from bent to extended conformations. Immunity 2006;25:583–594. [PubMed: 17045822]
40. Salas A, Shimaoka M, Chen S, Carman CV, Springer T. Transition from rolling to firm adhesion is regulated by the conformation of the I domain of the integrin lymphocyte function-associated antigen-1. J. Biol. Chem 2002;277:50255–50262. [PubMed: 12368274]
41. Alon R, Dustin ML. Force as a facilitator of integrin conformational changes during leukocyte arrest on blood vessels and antigen-presenting cells. Immunity 2007;26:17–27. [PubMed: 17241958]
42. Li R, Mitra N, Gratkowski H, Vilaire G, Litvinov R, Nagasami C, Weisel JW, Lear JD, DeGrado WF, Bennett JS. Activation of integrin $\alpha_{IIb}\beta_3$ by modulation of transmembrane helix associations. Science 2003;300:795–798. [PubMed: 12730600]
43. Takami M, Herrera R, Petruzzelli L. Mac-1-dependent tyrosine phosphorylation during neutrophil adhesion. Am. J. Physiol 2001;280:C1045–C1056.

44. Pluskota E, Woody NM, Szpak D, Ballantyne CM, Soloviev DA, Simon DI, Plow EF. Expression, activation, and function of integrin $\alpha_M\beta_2$ (Mac-1) on neutrophil-derived microparticles. Blood 2008;112:2327–2335. [PubMed: 18509085]

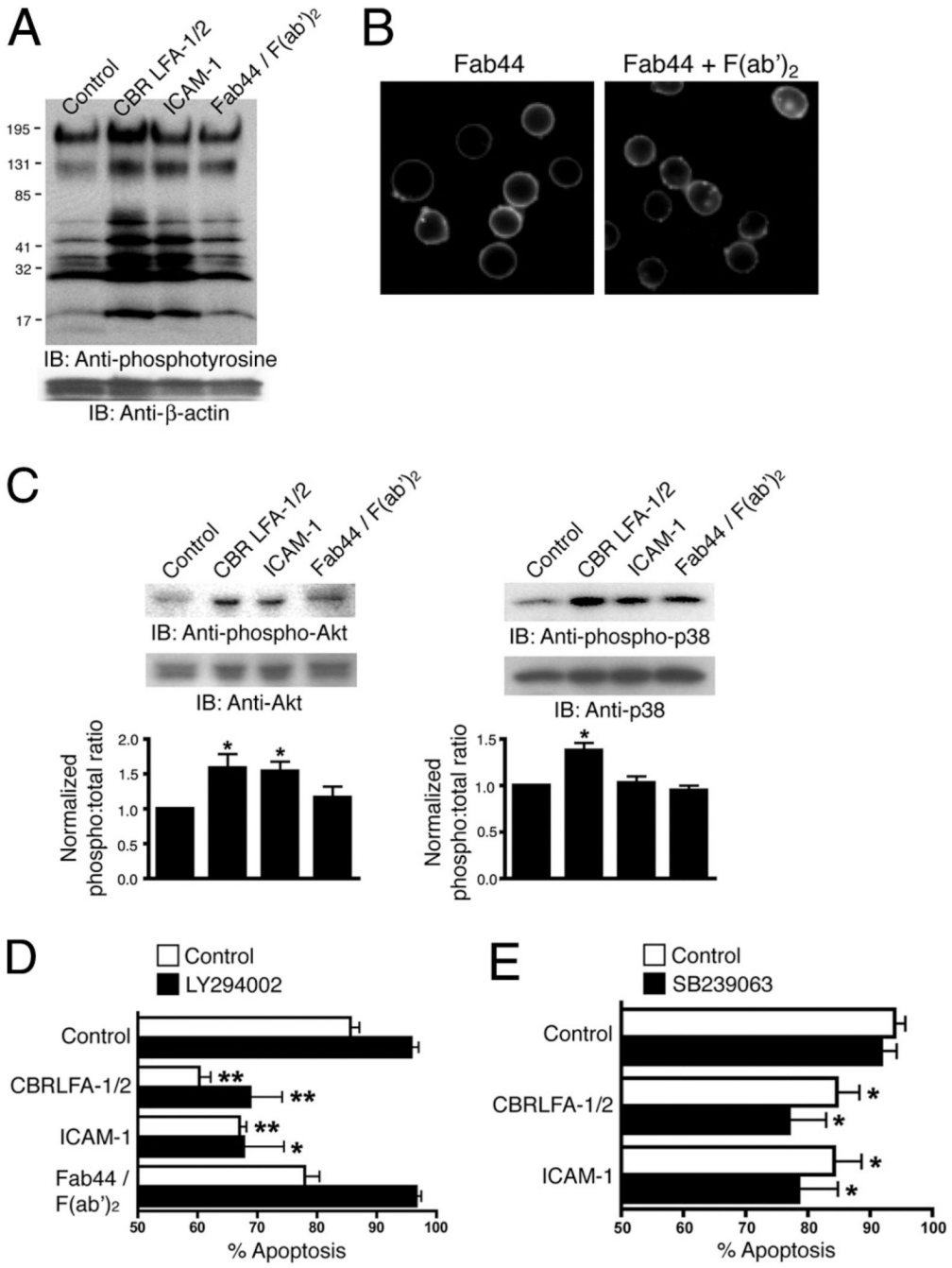

FIGURE 1.

A and *C*, PMN were treated at 37°C for 15 min with 10 μg/ml CBR LFA-1/2 or ICAM-1, both in the presence of 1 mM $MnCl_2$ or with anti-α_M Fab (Fab44) and secondary $F(ab')_2$ to induce Mac-1 clustering. For cells treated with CBR LFA-1/2, anti-α_M Fab fragments at a concentration of 50 μg/ml were used to block potential ligand binding. In *A*, immunoblots of whole-cell lysates were probed for the presence of tyrosine-phosphorylated proteins and for β-actin as a protein loading control. In *C*, immunoblots were probed for phosphorylated (phospho-p38; pThr180/pTyr182) and total p38, or for phosphorylated (phospho-Akt; pThr308) and total Akt. Western blot results from two experiments were quantified using ImageJ software and were normalized according to the control treatment. *B*, Unstimulated

PMNs were incubated at 37°C for 15 min with FITC-conjugated anti-α_M Fab44 (5 μg/ml) in the absence (*left*) or presence (*right*) of secondary F(ab′)$_2$ (2.5 μg/ml) to induce Mac-1 clustering. *D* and *E*, PMN were treated with 1 mM $MnCl_2$, 10 μg/ml CBR LFA-1/2 Fab and 10 μg/ml anti-α_M Fab (Fab44), 1 mM $MnCl_2$ and 200 μg/ml ICAM-1, or 5 μg/ml anti-α_M Fab (Fab44) and 2.5 μg/ml secondary F(ab′)$_2$ to induce Mac-1 clustering. Cells were pretreated for 15 min with or without 40 μM LY294002 or 2 μM SB239063. After incubation at 37°C for 16 h, cells were labeled with FITC-conjugated annexin V to detect apoptotic PMNs. Data are means ± SEM from three (*D*) or five (*E*) experiments performed in duplicate, and are expressed as percent of annexin V-positive cells. Significantly different from control (**, $p < 0.01$; or *, $p < 0.05$).

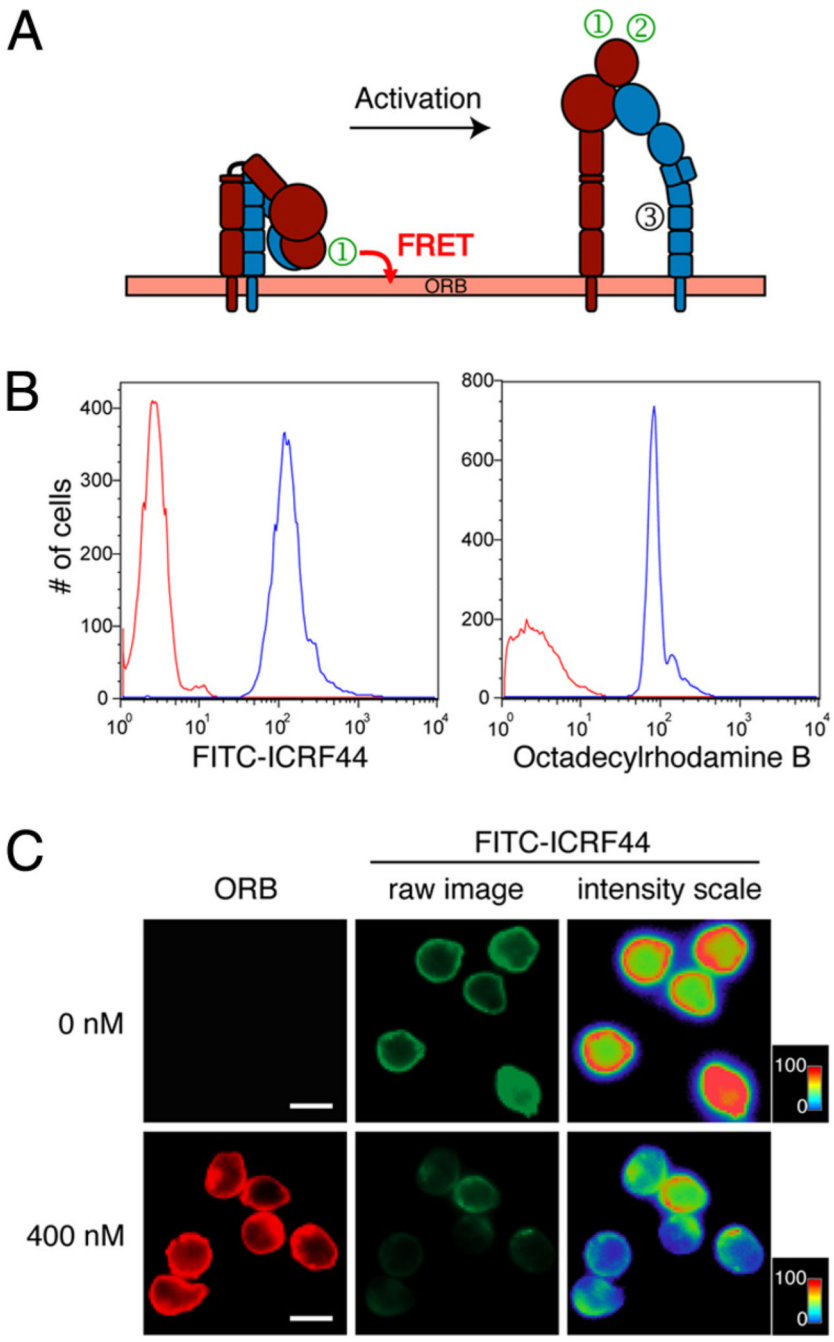

FIGURE 2.

A, Schematic depicting the loss of FRET between FITC-conjugated mAbs and ORB membrane dye during extracellular domain extension. The Abs used were: 1, FITC-ICRF44; 2, FITC-CBRM1/5; and 3, CBR LFA-1/2. *B*, PMNs labeled with FITC-ICRF44 and ORB (blue trace) or IgG1 isotype control (red trace) were analyzed by flow cytometry. *C*, PMN labeled with FITC-ICRF44 and then incubated with or without 400 nM ORB were imaged by immunofluorescence microscopy. *Far right*, intensity of the FITC signal converted to a rainbow scale. Bar, 10 μm.

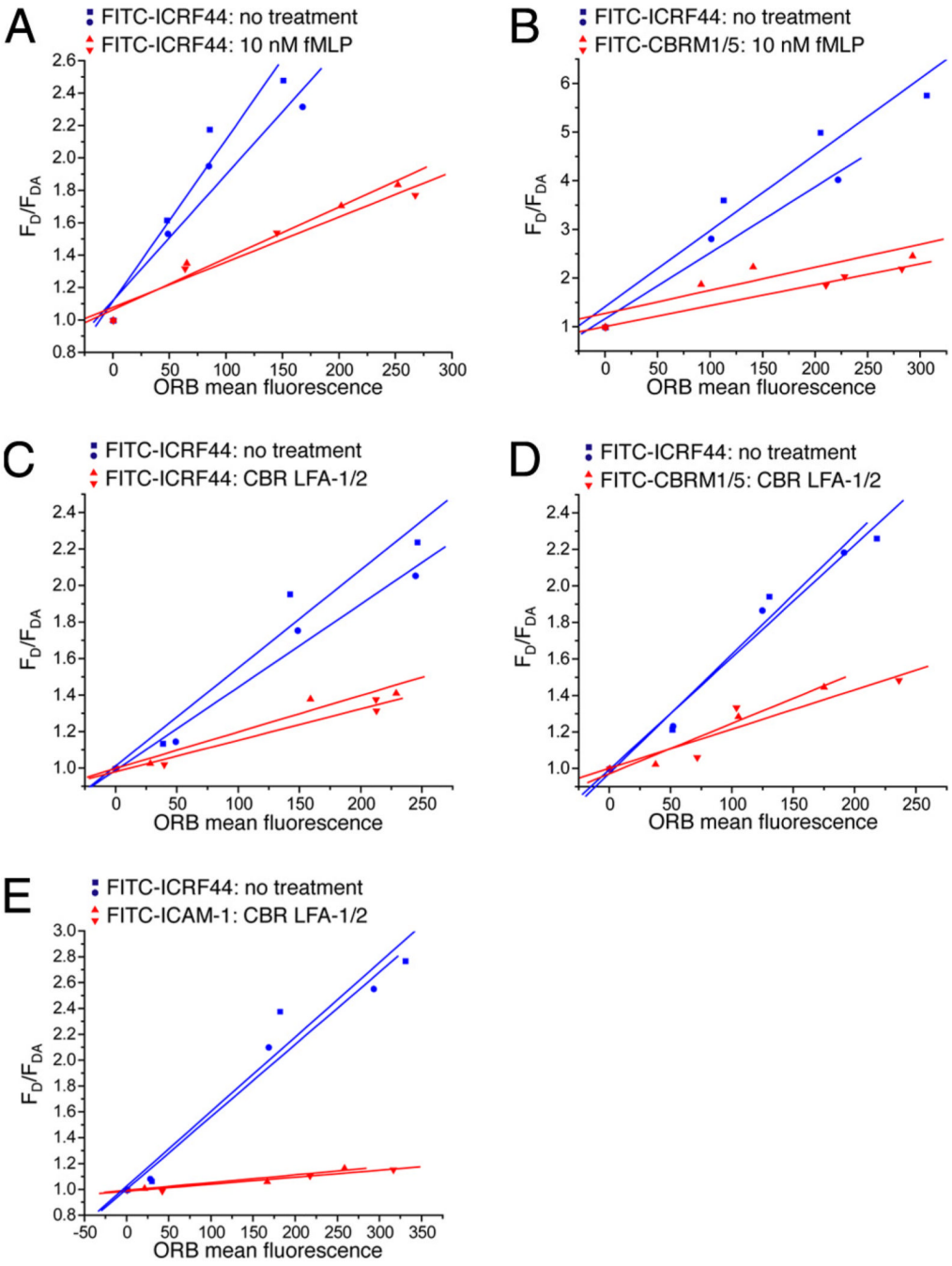

FIGURE 3.

PMN were stimulated with or without 10 nM fMLP (*A* and *B*) or with 1 mM $MnCl_2$ and 10 μg/ml CBR LFA-1/2 mAb (*C–E*) for 15 min. Unstimulated cells were labeled with FITC-ICRF44, and stimulated cells were labeled with FITC-ICRF44 (*A* and *C*), FITC-CBRM1/5 (*B* and *D*), or FITC-ICAM-1 (*E*). Cells were then incubated with 0, 75, 200, or 400 nM ORB and then analyzed by flow cytometry. Each plot consists of measurements from a single blood donor, with each condition being performed in duplicate (two curves per condition). Data are plotted as the fraction of the donor mean fluorescence intensity in the absence of acceptor fluorophores to that in the presence of the measured fluorescence acceptor (Equation 1).

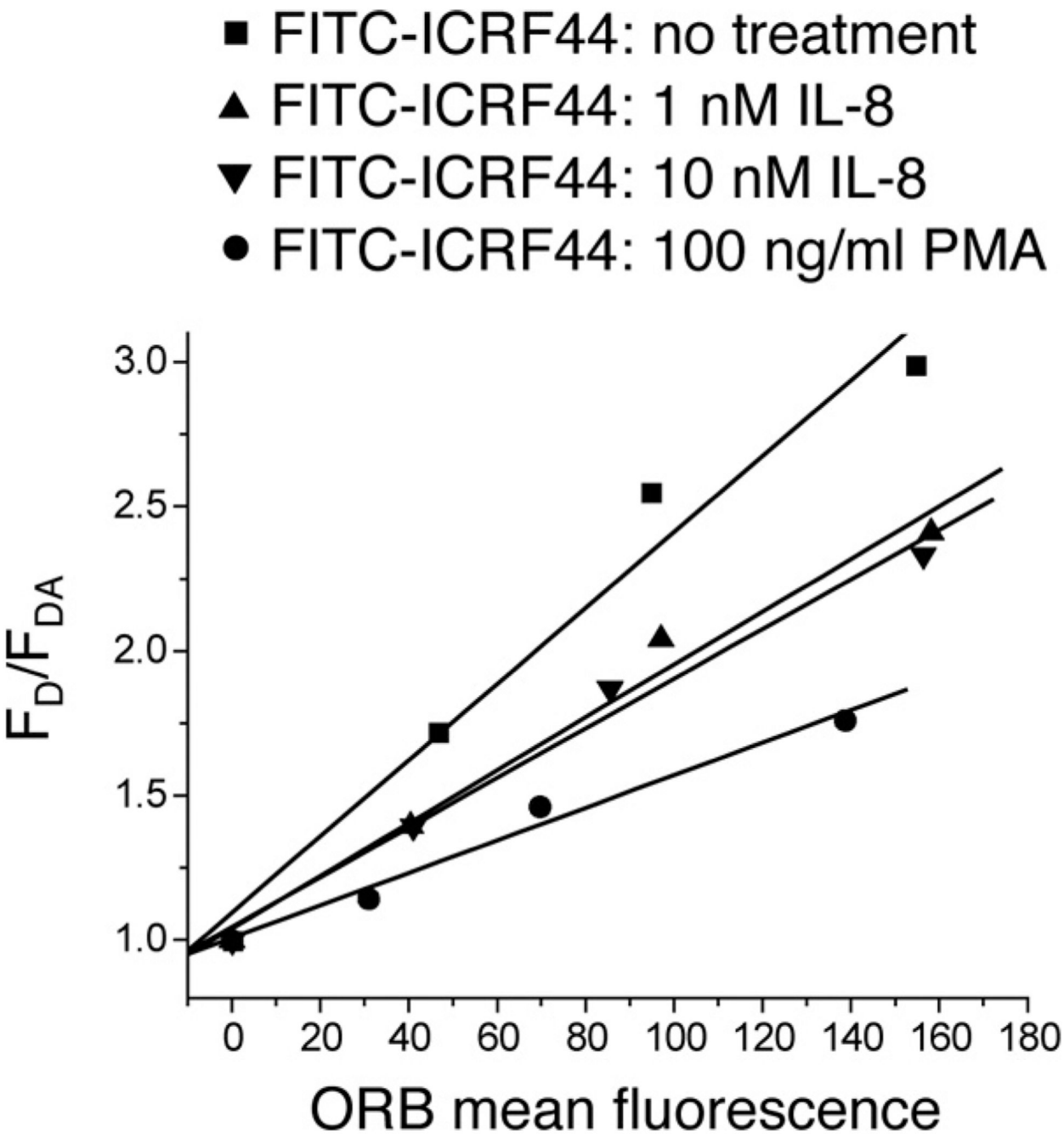

FIGURE 4.

Untreated PMN or PMN treated with 1 or 10 nM IL-8 or 100 ng/ml PMA were labeled with FITC-ICRF44 mAb. Cells were incubated with ORB as described in Fig. 3 and then analyzed by flow cytometry. Data are plotted as described in Fig. 3.

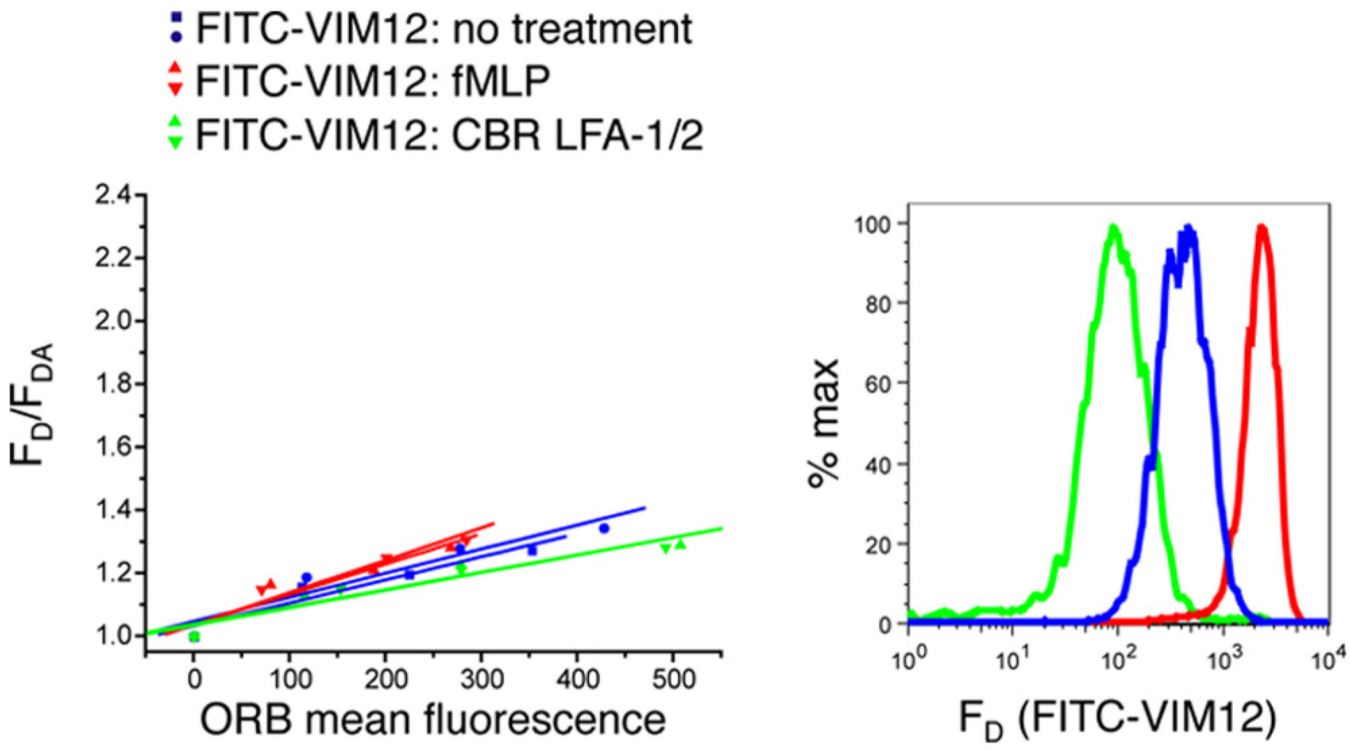

FIGURE 5.

Untreated PMN or PMN treated with 10 nM fMLP or 1 mM $MnCl_2$ and 10 μg/ml CBR LFA-1/2 mAb and then labeled with FITC-VIM12 mAb. Cells were incubated with ORB as described in the legend to Fig. 3 and then analyzed by flow cytometry. Data are plotted as described in Fig. 3.

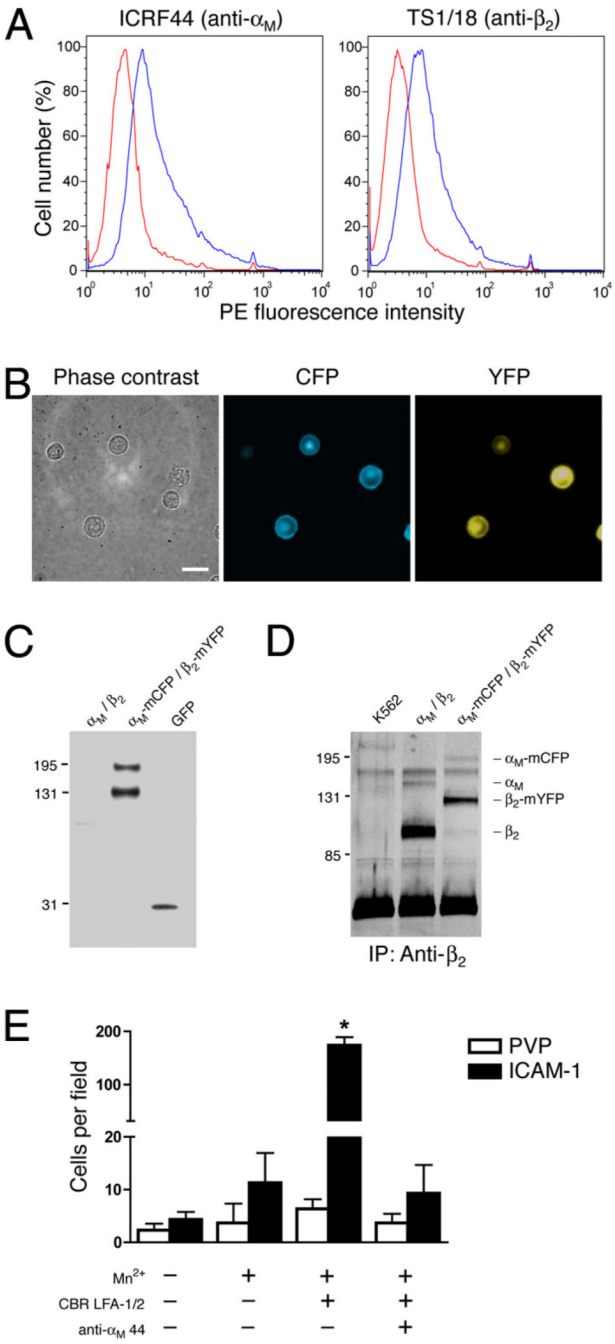

FIGURE 6.

A, K562 cells expressing α_M-mCFP and β_2-mYFP were labeled with anti-α_M ICRF44 mAb, anti-β_2 TS1/18 mAb, or IgG1 isotype mAb (red trace), followed by PE-conjugated secondary Abs. Cells were analyzed by flow cytometry. *B*, K562 cells expressing α_M-mCFP and β_2-mYFP were visualized under phase contrast and immunofluorescence microscopy. *C*, Whole-cell lysates from K562 cells expressing α_M-mCFP and β_2-mYFP were analyzed by immunoblotting using an anti-GFP polyclonal Ab. *D*, Mac-1 was immunoprecipitated from K562 cells, K562 cells expressing wild-type α_M and β_2, and K562 cells expressing α_M-mCFP and β_2-mYFP using the anti-β_2 CBR LFA-1/2 mAb. Proteins were separated on a 7.5% SDS-PAGE gel and then analyzed by silver staining. *E*, K562 cells expressing α_M-

mCFP and β_2-mYFP were allowed to adhere to tissue culture plastic coated with ICAM-1 or PVP, as a control, in the presence or absence of 1 mM $MnCl_2$, 10 μg/ml CBR LFA-1/2 mAb, and anti-α_M clone 44 mAb. After a 30-min incubation, nonadherent cells were washed away, and the number of adherent cells per field was counted. Data are presented as mean ± SEM from one of three independent experiments. *, Significantly different from control ($p < 0.01$).

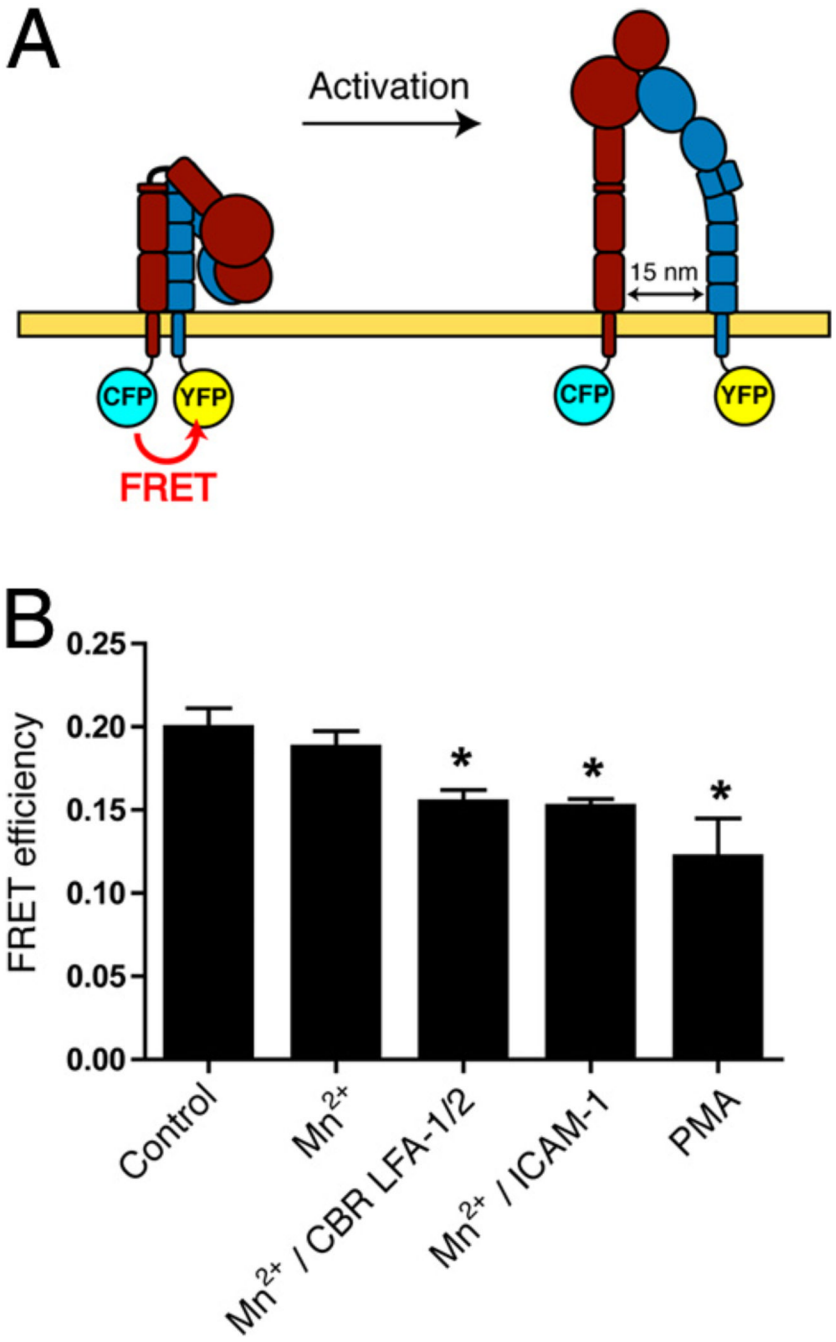

FIGURE 7.

A, Schematic depicting the loss of FRET between α_M-mCFP and β_2-mYFP during Mac-1 cytoplasmic tail separation. *B*, K562 cells expressing α_M-mCFP and β_2-mYFP were treated with 1 mM $MnCl_2$ in the absence or presence of 10 μg/ml CBR LFA-1/2 Fab or 200 μg/ml ICAM-1, or with 100 nM PMA. CFP and YFP images were captured of individual cells before and after photobleaching of the YFP signal. FRET efficiency was calculated as described in *Materials and Methods*. *, Significantly different from control ($p < 0.05$).